

Dislocation Energies in NaCl†

H. B. HUNTINGTON AND J. E. DICKEY, *Rensselaer Polytechnic Institute, Troy, New York*

AND

ROBB THOMSON, *University of Illinois, Urbana, Illinois*

(Received June 30, 1955)

The energies for both screw and edge dislocations in rock salt have been investigated. The effect of elastic anisotropy has been incorporated into the contribution from the region outside the core. Detailed calculations have been carried out for the energies of the cores themselves as a function of radius, and joined smoothly to the curves of the elastic theory. The core calculations are based on the Born-Mayer model and employ the formulas of Madelung for the potentials of rows of uniformly spaced charges.

For dislocations in the observed plane of slip (110), the constant term associated with the core energy is 1.0×10^7 ev/cm more for the edge than for the screw. Approximate calculations show this term to be appreciably larger for the edge dislocation in the (100) plane. Also, there appears to be large lattice potential barrier for dislocation motion in this plane arising from anion closed shell repulsion. This result may explain why these planes, though close packed, are generally not active in glide for alkali halides. The stability of dislocations with Burger vector longer than the minimum lattice translation is investigated. The possibility of hollow dislocations is also considered.

I. INTRODUCTION

THOUGH the treatment of dislocations within the framework of isotropic elastic theory has proved very fruitful in the past, there has been an increasing need recently to develop specific models for particular materials, which would be detailed enough to take into account the nonelastic distortions in the dislocation core region and the intrinsic anisotropy of the crystal elasticity. The alkali halides present obvious advantages for such a study. From the standpoint of theory a simple and reasonably satisfactory model exists in terms of point charges and short-range, ion-core repulsions which can account quite well for cohesion and for some of the elastic properties. From the standpoint of experiment the slip pattern is well known, namely in the [110] direction on the (110) planes, but one wonders why slip is not encountered along the close-packed (100) planes, as for the thallium salts and occasionally for AgCl, which shows pencil glide. Also, one is hopeful that a detailed study might throw light on the greater brittleness of alkali halides as compared to the silver salts.

We have calculated the core energies of certain dislocations on the basis of the simple force model. Initially the ion rows are arranged in accord with the isotropic elastic solution, and displacements are allowed to relax to minimize the stored energy. Such a procedure was applied by one of us¹ to the edge dislocation for slip in the (110) plane several years ago. More recently, an analogous calculation for the screw dislocation has been made by another of the authors.² The energies of various dislocations in the elastic region outside the cores have been calculated by the third author (R.T.),

taking into account the anisotropy of the crystal. From this last it has been possible to draw some conclusions about the stability of dislocations with Burgers vector longer than the shortest translation vector of the lattice. The possibility of "hollow" dislocations is also briefly considered.

II. ELASTIC STRAIN ENERGY OF DISLOCATIONS IN NaCl

In this section, we shall calculate the elastic energy of formation of various types of dislocations in NaCl. We shall assume that the crystal is a continuum, and that the strains are small, say less than ten percent. The core represents just that region near the center of the dislocation where neither of these assumptions is justified, and is dealt with separately. The total energy is, of course, the sum of the two contributions.

Anisotropic elasticity has traditionally been considered to be intractable because of the large mathematical difficulties to be faced. Since the problem has received added attention, general methods have been devised for the treatment of straight dislocations in arbitrary media.^{3,4} The elastic calculations in this paper are based on the techniques of Eshelby, Read, and Shockley.³

A. (110) Slip Planes

The experimental evidence available shows that the (110) planes in NaCl have a special place with regard to slip. Apparently under certain conditions other planes may be active also, but recent work⁵ confirms that at room temperature the (110) planes are the principal active slip planes, and so proves that dislocations are initially present on these planes. (Dommerich⁶ has

† This work was supported in part by the United States Air Force.

¹ H. B. Huntington, *Phys. Rev.* **59**, 942 (1941).

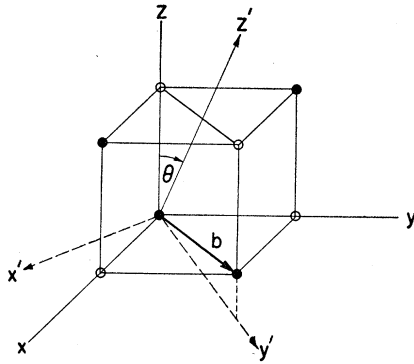
² J. E. Dickey, M.S. thesis, Rensselaer Polytechnic Institute (unpublished).

³ Eshelby, Read, and Shockley, *Acta Met.* **1**, 251 (1953).

⁴ A. Seeger and G. Schook, *Acta Met.* **1**, 519 (1953).

⁵ P. L. Pratt, *Acta Met.* **1**, 103 (1953).

⁶ S. Dommerich, *Z. Physik* **90**, 189 (1934).

FIG. 1. $(1\bar{1}0)$ slip plane in NaCl.

reported that wetted crystals can glide on (100) planes with a critical shear stress which is approximately three times that observed for (110) planes.) We shall thus begin with a discussion of the elastic strain energy of dislocations on (110) slip planes.

Figure 1 shows the situation in the $(1\bar{1}0)$ slip plane. The unprimed axes represent the cubic coordinate system in NaCl; the primed axes are used for the discussion of a dislocation in the $(1\bar{1}0)$ plane. The (straight) dislocation line is assumed to lie along the z' direction; hence both strain and stress are functions of x' and y' exclusively. The direction of slip in NaCl is also a $[110]$ direction and is indicated in the figure by the Burgers vector b —the shortest distance between like atoms. As the z' axis is rotated from the z direction to the b direction (always in the $(1\bar{1}0)$ plane), the dislocation line gradually changes its character from pure edge to pure screw type.

One of the features of anisotropic elasticity theory might be re-emphasized here. When the Burgers vector is parallel to the dislocation line and points in the z' direction in a crystal of low symmetry, the displacement is not necessarily in the z' direction also, i.e., the dislocation is not a simple screw. A similar result follows when the Burgers vector is perpendicular to the line of the dislocation; the displacement of material is not necessarily normal to the z' direction. In the case of NaCl, however, when z' is either in the z direction or the b direction, the symmetry in the $x'y'$ plane is great enough to ensure the usual pure edge in the first case and pure screw in the second. In the intermediate case, where $\theta \neq 0, \pi/2$, the situation is more complicated than if the material were isotropic, and one does not obtain a simple decomposition into pure edge and pure screw components corresponding to normal and parallel components of the Burgers vector. In order to apply the methods of Eshelby *et al.*, one needs to transform the elastic constants from those given with respect to the xyz system of coordinates to the values suitable to the coordinate system $x'y'z'$. The elastic constants are the components of a fourth-order tensor, and their components in the new coordinate system are given by

repeated application of formulas given in the standard references on elasticity.⁷

Calculations have been made with two sets of elastic constants. One set was taken at 80°K by Rose,⁸ and the other set was taken at 1000°K by Hunter and Siegel.⁹ It is assumed that 1000°K is a typical temperature of annealing, and probably represents the situation during the time that the dislocations have a chance to find their most favorable configuration. The low-temperature values are reasonably valid for a large-temperature interval, from probably zero to several hundred degrees. The results of Hunter and Siegel show an appreciable variation from the low-temperature values beginning at approximately 300–400°K. The elastic constants used are as follows:

80°K: $C_{11}=5.76 \times 10^{11}$ dynes/cm², $C_{12}=1.17 \times 10^{11}$ dynes/cm², $C_{44}=1.33 \times 10^{11}$ dynes/cm.

1000°K: $C_{11}=2.429 \times 10^{11}$ dynes/cm², $C_{12}=1.070 \times 10^{11}$ dynes/cm², $C_{44}=1.000 \times 10^{11}$ dynes/cm.

If τ_{ij} is the elastic stress tensor and b_i is the Burgers vector, it can be shown that the elastic strain energy is

$$E = \frac{1}{2} \int \tau_{ij} b_i ds_j, \quad (1)$$

where the integral is a surface integral to be taken over any regular surface bounded by the dislocation "loop." In our case, we consider a single dislocation line imbedded in a large crystal, so that the boundary of the surface in question is made by the dislocation line and the surface of the crystal. No attempt has been made to take account of the boundaries of the crystal in a detailed way. Indeed, if there were only one dislocation in a finite crystal, the stress would have to be relaxed on all boundaries, and small correction terms would thereby be added to the stress configuration near the boundaries themselves. It should be noted that stress relaxation actually destroys one of the basic assumptions—that all the stress and strain components are functions independent of z —because the addition of small stresses near the ends of the crystal where the dislocation breaks the surface destroys the property of plane strain which is always assumed. In this work we assume that the density of dislocations is sufficiently low and random that we can simply use the stress dis-

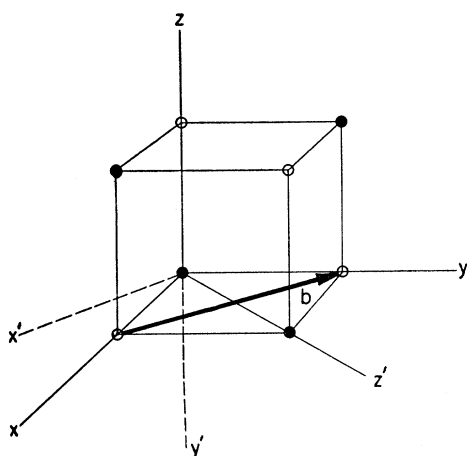
TABLE I. Elastic strain energy of dislocations on (110) slip planes.

θ	0°	10°	20°	30°	40°	50°	60°	70°	80°	90°
E_{80}	0.508	0.500	0.490	0.465	0.441	0.424	0.410	0.399	0.388	0.385
$\ln(R/r_0)$										

⁷ W. Voigt, *Lehrbuch der Kristallphysik* (B. G. Teubner, Leipzig, 1910); W. G. Cady, *Piezoelectricity* (McGraw-Hill Book Company, Inc., New York, 1946).

⁸ F. C. Rose, *Phys. Rev.* **49**, 50 (1936).

⁹ L. Hunter and S. Siegel, *Phys. Rev.* **61**, 84 (1942).

FIG. 2. (001) slip plane, $[\bar{1}10]$ Burgers vector.

tribution of an infinite body and arbitrarily cut off integrals at some distance roughly corresponding to the mean distance between dislocations in the real crystal. In an actual well-annealed crystal, the dislocations are probably far from randomly distributed, and, because of the long-range nature of the stress distribution, a particular model may give somewhat different energy values than the ones we have derived.

The calculations were essentially numerical in form, and, with low-temperature elastic constants, were performed for each ten-degree increment in θ from 0° to 90° . The results show a monotonic transition in the value of the energy between the edge ($\theta=0$) and the screw ($\theta=\pi/2$). The results are shown in Table I. E_{80} is given in electron volts per atomic distance along the dislocation line. For NaCl, "atomic distance" is 2.81×10^{-8} cm. The quantity R is the outer cut-off radius discussed above; r_0 is the inner cut-off radius, and corresponds to the limit of elasticity theory; in other words, r_0 is the size of the core of the dislocation.

The results can be approximately represented with a simple cosine variation,

$$E_{80} = (0.454 + 0.061 \cos 2\theta) \ln(R/r_0), \quad (2)$$

with a maximum error of about two percent, which is not much greater than the error of the calculation itself.

We have only made calculations of elastic energy for two values of θ , $\theta=0$ and $\pi/2$, for the temperature 1000°K . We assume that in this case also the variation between the screw and the edge is simple, and using the cosine law above, we find

$$E_{1000} = (0.214 + 0.032 \cos 2\theta) \ln(R/r_0). \quad (3)$$

In a later section, the contribution of the cores of edge and screw dislocations will be added to these values to yield the final strain energy.

B. Elastic Calculations on Other Planes

In order to provide a comparison with other slip planes, we have made calculations for the situation

illustrated in Fig. 2. The Burgers vector remains the same as before, but the slip plane is (001). The calculations reported above, when repeated for this case with the same temperatures as before, give for the energy of the edge dislocation,

$$E_{80} = 0.456 \ln(R/r_0), \quad E_{1000} = 0.267 \ln(R/r_0). \quad (4)$$

Note that the corresponding screw dislocation in this case is precisely the same as for the (110) slip planes discussed earlier.

Referring either to Fig. 1 or Fig. 2, one sees that the (110) and (001) planes are only two out of an infinite family of planes which contain the same Burgers vector b . For the sake of completeness, one would like to know the energy of dislocations in these planes where slip is not observed. We have made calculations of the elastic energy of pure edge dislocations in planes inclined at various angles to the observed slip plane. In Fig. 1, if one lets the Burgers vector point in the x' direction, then as θ varies from 0 to $\pi/2$, the slip plane varies from (110) to (001). The elastic energy of pure edge dislocations as a function of slip plane is given in the following Table II for the temperature 80°K . Note that the variation in the elastic energy is again monotonic, and is quite small. We will show later that the core energy probably overbalances the difference in elastic energy shown here between the (110) and (001) slip planes. Since core calculations have been made only for the extreme (110) and (001) types, one cannot predict the actual variation between the two extremes, except to say that the variation in energy of the core is the dominant factor.

The screw dislocation corresponding to each edge dislocation in the above table is in all cases the same, namely the one discussed in Sec. A.

There remains the question of how the dislocation energy varies as one goes from pure edge to pure screw in one of these planes. Only one such calculation has been made, a half-edge, half-screw dislocation whose slip plane is (010). This particular dislocation is discussed later, and its elastic energy is given in Eq. (7).

It is interesting to consider the possibility of other types of Burgers vectors than the $[110]$ in NaCl, even though there seems to be no experimental evidence for them. Calculations of a screw and an edge dislocation with Burgers vectors of type $[002]$ were made with elastic constants appropriate for 80°K and 1000°K . The two types of dislocation considered are shown in Fig. 3.

TABLE II. Elastic energy of pure edge dislocations as a function of slip plane.

θ	0°	10°	20°	30°	40°	50°	60°	70°	80°	90°
$\frac{E_{80}}{\ln(R/r_0)}$	0.508	0.505	0.499	0.490	0.480	0.471	0.463	0.458	0.457	0.456

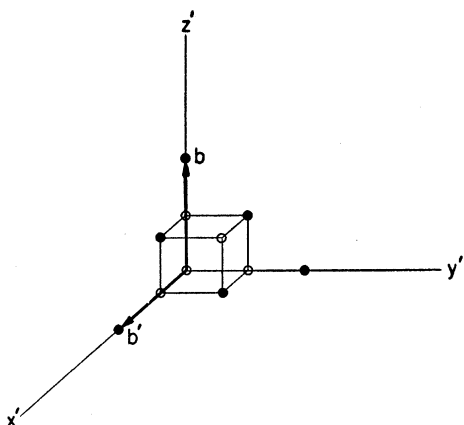
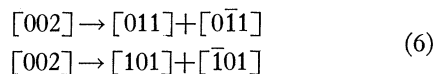


FIG. 3. Large dislocations. The figure shows one edge dislocation and one screw dislocation with the Burgers vectors $[002]$ and $[200]$, respectively. The edge dislocation has a slip plane (010) . The dislocation line, in each case, is in the z' direction.

The energies, in the same units as before, were:

$$\begin{aligned} \text{Edge: } E_{80} &= 1.013 \ln(R/r_0), & E_{1000} &= 0.492 \ln(R/r_0). \\ \text{Screw: } E_{80} &= 0.586 \ln(R/r_0), & E_{1000} &= 0.442 \ln(R/r_0). \end{aligned} \quad (5)$$

Note that in this case the dislocation Burgers vector reaction



may take place, in which the "large" dislocation breaks up into two component dislocations with the Burgers vectors $[0\bar{1}1]$ and $[011]$. If the energy of the two component dislocations taken together is smaller than the energy of the "large" dislocation, then the breakup

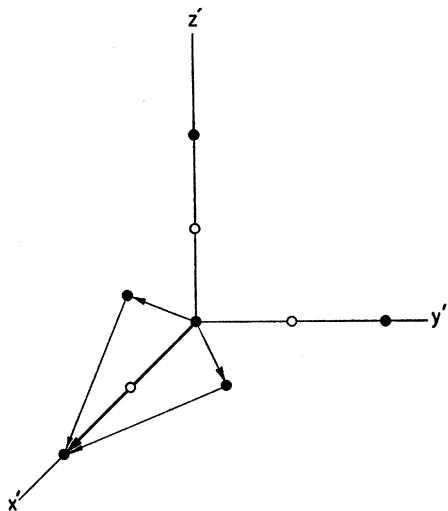
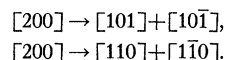


FIG. 4. Breakup of a "large" edge dislocation in a (010) slip plane. The Burgers vector of the large dislocation is $[200]$, and the line of the dislocation is in the z' direction. Two reactions are possible:



will take place spontaneously; otherwise the large dislocation, once formed, will be stable.

The details of the breakup process are shown in Figs. 4 and 5. In order to test the stability with respect to breakup, we need to know the energy of the decomposition product which has the Burgers vector $[101]$ and runs in the z' direction. We have here a half-edge, half-screw, dislocation whose slip plane is (010) . The elastic strain energy of this dislocation is given in the same units as before by

$$E_{80} = 0.401 \ln(R/r_0), \quad E_{1000} = 0.233 \ln(R/r_0). \quad (7)$$

(Note that in both cases these energies are intermediate in value between the pure edge and screw types.) The stability of the two types of dislocations is best demonstrated in Table III. The first column gives the type of large dislocation, either screw or (010) edge. The third column of Table III gives the elastic strain

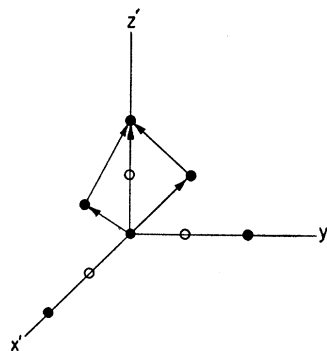
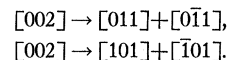


FIG. 5. Breakup of a "large" screw dislocation. The Burgers vector of the large screw dislocation is $[002]$. Two possible decompositions are possible:



energy divided by the logarithm term. The large dislocation is stable with respect to breakup if the number in column 4 is larger than the number in column 3. The log factor for the large dislocation is approximately the same as the log factor for the small component. For the large dislocation, r_0 is about two times the r_0 of the small dislocation, because the cutoff has to be taken in each case where the strain is small. However, when the large dislocation breaks up into two, the free area for each dislocation has been effectively cut in half, and hence R for the large dislocation is also about two times the R for the small one. Note that at both the low and high temperatures, the edge is apparently unstable with respect to breakup into either type of component. The screw at first sight seems to be stable. However, since the two energies are so close together, the core energy will be the decisive quantity. One would expect the core energy of the large core to be slightly larger than the combined core energy of the components. Since screw elastic energies per unit length are less than those of

edge dislocations, it is unlikely that any other large dislocations will be more stable than [002] screws.

III. DISLOCATION CORE ENERGIES IN NaCl

To study the dispositions of the atoms in the core region and the associated stress energy, it was advisable to choose a substance where the forces between the atomic constituents were well known and of short range type. The alkali halides are well suited to the problem since one has to deal with the electrostatic forces and, at close range, the repulsive forces of the closed shells. The electrostatic forces are short range also except where logarithmic potentials from rows of ions of the same sign are involved.

A. Edge Dislocation: (110) Slip Plane

The first step in the procedure was to use the displacements predicted by the isotropic elastic solution, even in the core region where they were no longer valid. If the x axis is taken along the slip direction and the y axis along the normal to the slip plane, then u and v the respective components of the displacements along

TABLE III. Stability of large and small dislocations.

Parent type	Temperature	$\frac{E_{\text{large}}}{\ln(R/r_0)}$	$\frac{2(E_{\text{small}})}{\ln(R/r_0)}$	Component type	Stability
Screw	1000°K	0.442	0.466	Mixed (100)	?
Screw	80°K	0.586	0.802	Mixed (100)	Stable
Edge	1000°K	0.492	0.492	(110) edge	Unstable
Edge	1000°K	0.492	0.466	Mixed (100)	Unstable
Edge	80°K	1.016	1.016	(110) edge	Unstable
Edge	80°K	1.016	0.802	Mixed (100)	Unstable

these axes are given by

$$u = \frac{b}{2\pi} \left[\tan^{-1}(y/x) + \left(\frac{\lambda + \mu}{\lambda + 2\mu} \right) \frac{xy}{r^2} \right], \quad (8)$$

$$v = \frac{b}{2\pi} \left[-\frac{\mu}{\lambda + 2\mu} \log r + \left(\frac{\lambda + \mu}{\lambda + 2\mu} \right) \frac{y^2}{r^2} \right],$$

where b is the slip distance and λ and μ are the familiar elastic Lamé constants for an isotropic substance. This sets up a dislocation where the material is compressed for $y > 0$ and extended for $y < 0$.

In developing the elastic displacements for the various ion rows, it was found expedient to arrange them symmetrically about the yz -plane perpendicular to the direction of slip. Two such arrangements were considered: Configuration I with the symmetry plane passing through two adjacent ion rows on opposite sides of the dislocation center (Fig. 6), and Configuration II with the plane of symmetry half way between the four ion rows nearest the dislocation center (Fig. 7). For slip on the (110) plane the edge dislocations lie parallel to [001] and perpendicular to the slip direction. In the [001] direction, the signs of the ions alternate.

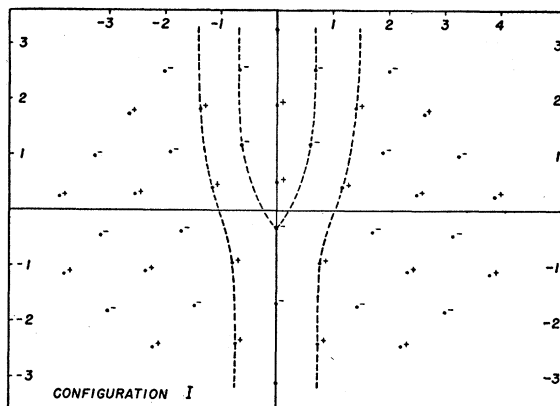


FIG. 6. Edge dislocation for slip in (110) plane—Configuration I.

The electrostatic potential of a row of alternately charged particles, spaced a distance a apart is given by¹⁰

$$\frac{2e}{a} \sum_{l=1}^{\infty} i\pi H_0 \left(\frac{i\pi l r}{a} \right) \cos \left(\frac{2\pi l z}{a} \right). \quad (9)$$

Here e is the magnitude of the charge per ion. Distance from the row is measured by r and distance in the direction of the row by z . For application to NaCl a is 2.81 Å. The H_0 is the Hankel function of zero order.

For the energy arising from the repulsion of closed shells a single expression was chosen to represent the interaction between next neighbor ions of opposite sign. The repulsion between like (negative) ions was neglected to keep the calculation as simple and, at the same time, as general as possible, in that the results would not appear as specific for a particular salt. By virtue of the equilibrium condition, the single force law could be written

$$W(x) = \frac{1}{6} \frac{e_p^2}{a^2} e^{-(x-a/\rho)}, \quad (10)$$

where α_m is the Madelung number for the NaCl

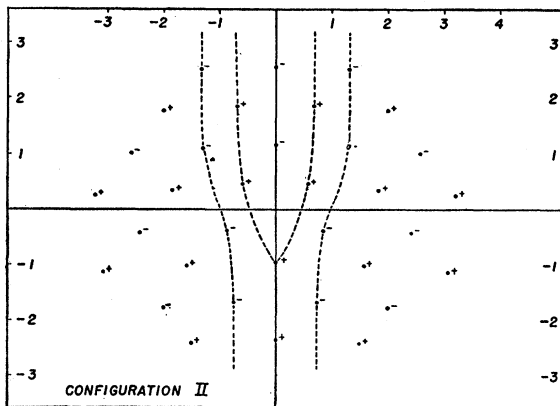


FIG. 7. Edge dislocation for slip in (110) plane—Configuration II.

¹⁰ E. Madelung, Physik. Z. 19, 524 (1918).

TABLE IV. Final positions of ions in core of edge dislocation in (110) plane.

		Configuration I					
s	0+	0-	2+	2-	4+	4-	6+
x/b	0	0	0.859	1.195	1.788	2.226	2.762
y/b	0.37	-0.29	0.29	-0.28	0.20	-0.32	0.17
$D(s)$	0	0	-0.141	0.195	-0.212	0.226	-0.238
		Configuration II					
s	1+	1-	3+	3-	5+	5-	
x/b	0.431	0.633	1.315	1.710	2.268	2.732	
y/b	0.34	-0.28	0.25	-0.30	0.19	-0.33	
$D(s)$	-0.069	0.133	-0.185	0.210	-0.232	+0.232	

structure and ρ is an empirical constant which appears in the Born-Mayer formula for the repulsion energy between closed shells and is here set at 0.325 A.

The positions of the ion rows for each of the two configurations were next adjusted to a closer approximation by requiring that the interaction of each row with its nearest neighbors and next nearest neighbors be minimized. The procedure was to begin with those rows nearest the center of the dislocation, where the elastic displacements would be most inaccurate, and proceed outward. Except for those rows directly adjoining the dislocation center the displacement corrections were small, of the order of 3 or 4 percent of the interatomic distance, a . The final disposition of the ion rows for both configurations is shown in Fig. 6 and Fig. 7, respectively.

In Table IV are given the final x and y coordinates of the ions directly above and below the slip plane in units of the Burgers vector, $b = \sqrt{2}a$, for both configurations. The ions are indexed by the s number, where $sb/2$ measures the distance to the right or left of the dislocation center at which the ion would be located if no strains were present. The plus or minus sign following the s number indicates whether the ion lies in the upper (compressed) or lower (expanded) half-plane. After the manner of Nabarro¹¹ we define a displacement function,

$$D(s) = x/b - s/2,$$

where $D(\pm\infty) = \mp \frac{1}{4}$ for the upper half-plane and $\pm \frac{1}{4}$ for the lower half-plane. The form of D gives the shape of the dislocation. It is usual to ascribe a "width" to the dislocation equal to the distance between the points at which D takes on one half its values at $\pm\infty$. Averaging between Configurations I and II, it appears that $|D|$ takes on the value $\frac{1}{8}$ just short of $x = 0.75b$, which gives a dislocation width of $1.5b$. This value is close to that found by Nabarro,¹¹ $b/(1-\sigma)$, where σ is Poisson's ratio and indicates a very compact dislocation. The work of Peierls and Nabarro has shown that the energy hill opposing the motion of a dislocation lying along a crystallographic direction decreases exponentially with increasing dislocation width. Consequently, Cottrell has expressed the viewpoint¹² that actual dislocations are

¹¹ F. R. N. Nabarro, Proc. Phys. Soc. (London) **59**, 257 (1947).

¹² A. H. Cottrell, *Progress in Metal Physics* (Butterworth Publications, London, 1949), Vol. I, p. 91.

probably broader than $b/(1-\sigma)$ if one is to account for the low observed yield stress in well annealed single crystals. The actual forms for such dislocations have been examined by Foreman, Jaswon, and Wood.¹³ It is somewhat disturbing to find this dislocation so compressed. The displacements arising from energy minimization have nevertheless broadened the dislocation appreciably.

The stored energy of the dislocation inside any cylinder coaxial with its center can be determined next from the results of minimizing the energy. (Minimization in general reduced the stored energy by about a factor of $\frac{1}{2}$.) One takes all the interaction energies between rows inside the cylinder and adds to it a half of the interaction energies between rows inside and outside the cylinder. In this way one obtains the stored energy content of cylinders containing a symmetric grouping of rows. In Configuration I, these groupings contained 2, 10, 20, and 24 rows respectively; for Configuration II, 6 and 18. In Fig. 8, the energy content of the cylinders is plotted in units of ev/plane vs the cylinder radius R . The radius of the equivalent cylinder is established by

$$\pi R^2 = na^2, \quad (11)$$

where n is the number of rows inside the cylinder. From this curve one could obtain the energy of the dislocation core ideally by fitting the curve with the formula

$$E(R) = A \ln(R/a) + B. \quad (12)$$

Actually, one uses instead the value for A , 0.508 ev

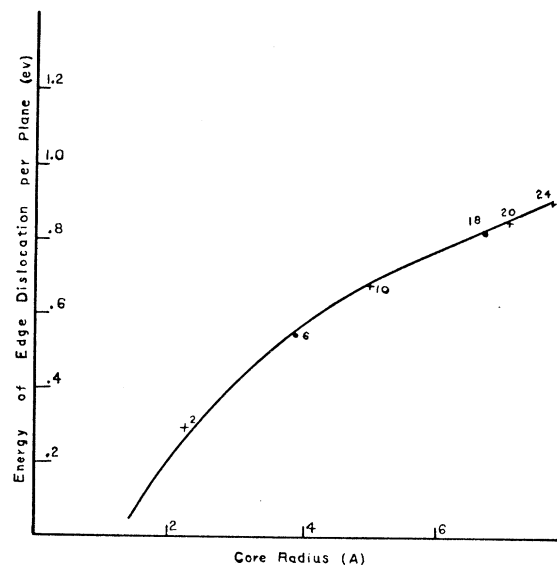


FIG. 8. Edge dislocation for slip in (110) plane—energy vs R . Plus signs refer to Configuration I, open circles to Configuration II; nearby numbers show how many ion rows inside cylinder of radius R . Smooth curve is plot of Eq. (12).

¹³ Foreman, Jaswon, and Wood, Proc. Phys. Soc. (London) **64**, 156 (1951); further modification in the Peierls-Nabarro dislocation will shortly be presented by one of us (H.B.H.).

per plane obtained from elastic considerations in Sec. A and fits at the point for greatest R , giving $B=0.392$ eV per plane. The solid line in Fig. 8 is the plot of Eq. (12). It fits the points very well, fortuitously so, because the simplified force model used here, with repulsion only between ions of opposite sign, does not accurately reproduce the elastic constants.

B. Screw Dislocation

The treatment of the screw dislocation likewise involves consideration of two distinct configurations, which we show as Configurations III and IV in Figs. 9 and 10 respectively. They correspond to a screw dislocation along the slip direction $[110]$, so that the ion rows are all composed of ions of the same sign. In Configuration III, the dislocation lies symmetrically at the center of a rectangular prism formed by alternative positive and negative ion rows at the corners. In Configuration IV the dislocation has moved a distance $b/2\sqrt{2}$ along the $[001]$ direction, as would occur for slipping in the (110) plane. It can be seen that the ion rows are arranged in an alternating rectangular array. Those rows marked by full circles have ions in the plane of the paper, those marked in broken circles have ions in planes above and below the plane of the paper. Individual ion rows will be designated by the numbers along the center lines with abscissa index coming first (e.g., 1, -3 denotes negative row at bottom of Fig. 9 with ions above and below the plane of the figure). The

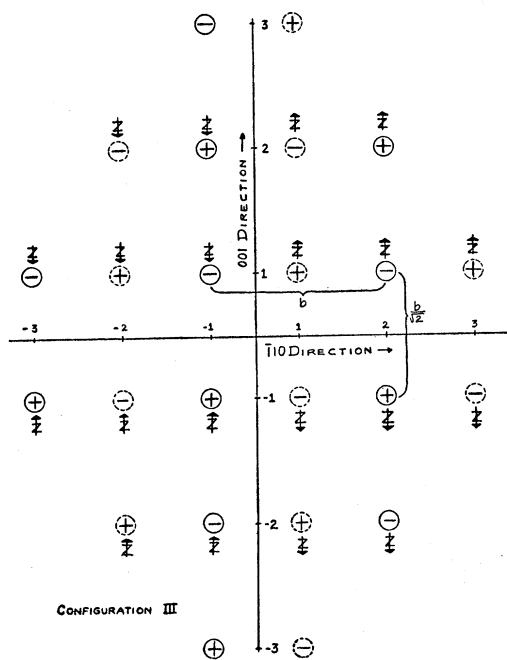


FIG. 9. Screw dislocation—Configuration III. Solid circles denote rows which initially had ion in plane of paper, dashed circles for rows with ions initially $b/2$ above and below the plane. Arrows with superimposed Z indicate direction of ϵ_z , the relaxation displacement perpendicular to the paper.

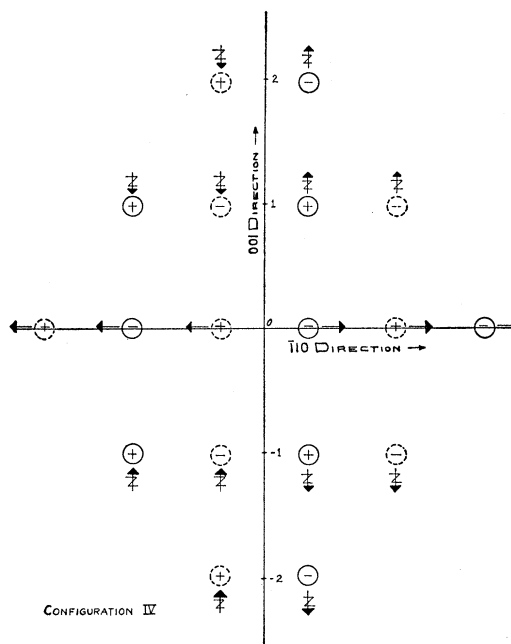


FIG. 10. Screw dislocation—Configuration IV. Same notation as Fig. 9. Outward displacement of ion rows denoted by simple arrow.

distance between rows in the $[\bar{1}10]$ direction is $b/2$, in the $[001]$ direction $b/\sqrt{2}$.

For the interaction energies between the rows the same ion-core repulsion expression, Eq. (10), is used as for the edge dislocation of the preceding section. This interaction is mainly important between rows separated by $b/2$ in the $[\bar{1}10]$ direction. Here every ion in one row is in contact with two ions in the adjoining row, one from the plane above and the other from the plane below. For the electrostatic interaction one uses again a formula due to Madelung¹⁰

$$V(z,r) = 4e/b \left[\sum_{l=1}^{\infty} K_0(2\pi lr/b) \cos(2\pi lz/b) - \frac{1}{2} \ln 2b/r \right] \quad (13)$$

for the potential at a point a distance r from a line of charges e spaced a distance b apart. The variable z is measured parallel to the line of like charges, with one of the charges at the origin.

The displacements caused by an elastic screw dislocation are simply

$$\epsilon_{ze} = b\theta/2\pi,$$

where we have taken θ to be measured counterclockwise from the $[\bar{1}10]$ direction and z is measured + up from the paper. Since the dislocation at this stage introduces only changes in z , the $\ln r$ terms in the electrostatic potential expression are unaffected and the calculation of the stored energy depends only on short-range interactions as before.

For Configuration III, it turns out that the relaxations are principally z -ward motions. These have been

indicated in Fig. 9 by arrows pointing up for motion up out of the plane of the paper and down for downward motion. The superscribed Z 's on the arrows indicate that they are not to be interpreted as motions in the plane. One complication is introduced by the radial symmetry about the dislocation which is higher than that for the previously treated case of the edge. Any upward z -motion for row 1,1 implies from symmetry a similar motion for $-1,-1$ and the reverse motion for $1,-1$ and $-1,1$. The principal interactions here are those parallel to the $[\bar{1}10]$ direction, $-1,1$ with $1,1$ and $-1,-1$ with $1,-1$. If ϵ_z is taken to be the upward motion of say $1,1$, then its value is to be determined by minimizing the energy of the central four rows,

$$2U(z_{-1,1}-z_{1,1}-2\epsilon_z; b/2) - 2U(z_{1,1}-z_{2,1}+\epsilon_z; b/2),$$

where $U(z; r)$ is written for the complete interaction function composed of $V(z, r)$ and the ion-core repulsions. Actually the optimum value for ϵ_z for just the central four rows proved to store too much energy in the rows farther out, and this complication made the precise determination of ϵ_z difficult. Therefore, three values for ϵ_z were chosen, $0.05b$, $0.06b$ and $0.07b$, and for each the optimum values were found for the z -displacements of the other rows. (The results appear later in Fig. 12.) The possibility of outward relaxation in the $[\bar{1}10]$ direction was also investigated after the manner described in the next paragraph, but it was found that there was no appreciable outward relaxation after a z -relaxation of $0.05b$. It is possible that simultaneous variation of ϵ_z and ϵ_r might have given a slightly lower energy minimum at appreciably different coordinates but the labor involved in such a program would have been very considerable. In Table V are given the values of the z displacements for the other ion rows of Configuration III, largely independent of ϵ_z for the central rows.

For Configuration IV, the outward radial displacement of $1,0$ and $-1,0$ is particularly important since z -displacements of these rows are ruled out by symmetry. Therefore the technique of investigating this relaxation, which requires some comment, will be discussed here. The variations with r of the first term in Eq. (13) for particular values of z was made available for reference in graphical form. The part of $V(z, r)$ involving $\ln r$ is more difficult to treat, since it is a long range interaction. One needs to know the change in potential energy of a rectangular array of line charges

TABLE V. Z -displacement for outer ion rows in a screw dislocation.

Ion row index Z -displacement, ϵ_z	Configuration III			
		2,1	1,2	3,1
	$0.06b$	$0.015b$	$0.03b$	$0.02b$
Ion row index Z -displacement, ϵ_z	Configuration IV			
	1,1	2,1	1,2	3,1
	$0.03b$	$0.02b$	$0.01b$	$\sim 0.02b$

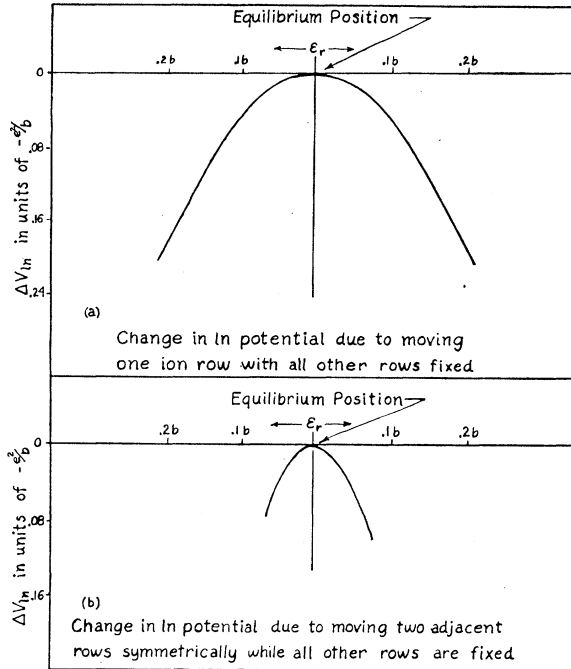


FIG. 11. Variation of \ln potentials with ϵ_r .

with alternating sign when one of the array is displaced from its equilibrium position in the direction of one of its neighbors. An expression for this quantity, valid for small displacements, is developed in Appendix I and displayed in Fig. 11(a). For application to the coupled motion of $1,0$ and $-1,0$ one needs also to take into account the mutual interaction of the two moving rows. The analytic expression for this interaction is equivalent to the formula for the interaction of two dipole line charges and is given as the second term in the expression below for the complete change in the logarithmic potentials

$$\Delta V_{\ln} = (-2e/b) \{ 4.756(\epsilon_r/b)^2 + \ln[(1+2\epsilon_r/b)^2/(1+4\epsilon_r/b)] \}. \quad (14)$$

ΔV_{\ln} is plotted in Fig. 11(b).

Here it is difficult to establish with precision the optimum value for ϵ_r for the whole dislocation by examining only the energy of $1,0$ and $-1,0$. For three values of ϵ_r , $0.05b$, $0.055b$, and $0.06b$, the corresponding optimum radial displacements for rows $2,0$ and $-2,0$ were $0.010b$, $0.011b$, and $0.012b$ respectively. The z -displacements of the other rows could be determined directly by minimization and are given in Table V.

For discussing the shape of the screw dislocation there appears to be no single parameter, such as the "width" which applies to the edge dislocation. However, the z -relaxations for Configuration III have altered it markedly from the symmetric dislocation of elastic theory. It is now anisotropic and the shear strain in the $(\bar{1}10)$ plane has been increased at the expense of the

strains in the (001) plane. This distortion tends to lower the barrier for dislocation motion in the (001) plane and conversely raise it for motion in the (110) plane. Again the radial motions of central rows of the Configuration IV tend to reduce the shear strain in the (001) plane and to spread out the dislocation along the $[110]$ direction.

The energy results for the screw dislocations are summarized in Fig. 12, where the presentation is closely analogous to Fig. 8 for the edge dislocation. For Configuration III, cylindrical groupings of 4, 12, and 24 rows give 3 values for R for which energy points are plotted for various ϵ_z . Here $R = (n/\pi\sqrt{2})^{1/2}a$. Likewise, Configuration IV gives 3 points for groupings of 2, 8, and 18 rows. The energy curves before relaxation are also shown and it can be seen that the total energy for the twenty innermost rows was decreased by relaxation in the case of Configuration IV by about 65%, in the case of Configuration III by about 35%. Fitting to an equation of the form of Eq. (12) one uses for the coefficient of the elastic term the value of 1.37×10^7 ev/cm found in Sec. A and finds for the constant term 0.38×10^7 ev/cm. These numbers in Eq. (12) give the smooth curve shown in Fig. 12.

C. Edge Dislocation for Slip in the (100) Plane

The elastic results of Sec. II raise a question as to how dislocation theory can account for the observed

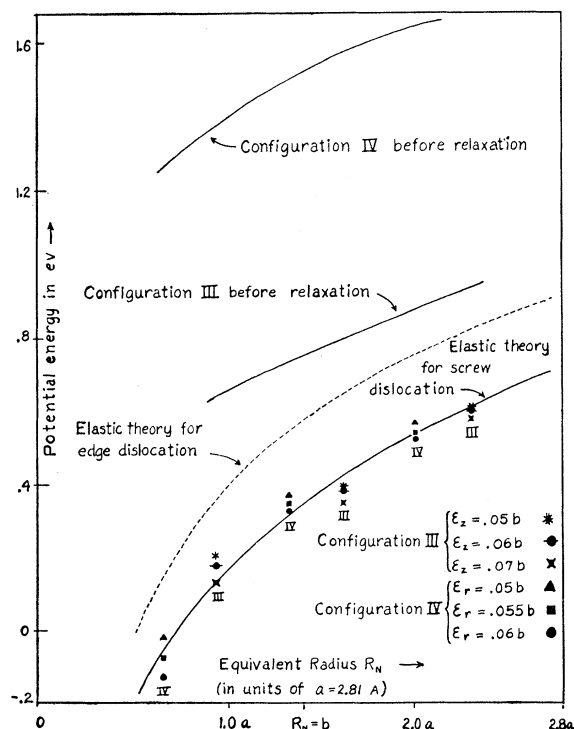


FIG. 12. Screw dislocation—energy vs R . Dotted line gives analogous curve for edge dislocation in (110) plane. Upper lines indicate approximate energies before relaxations.

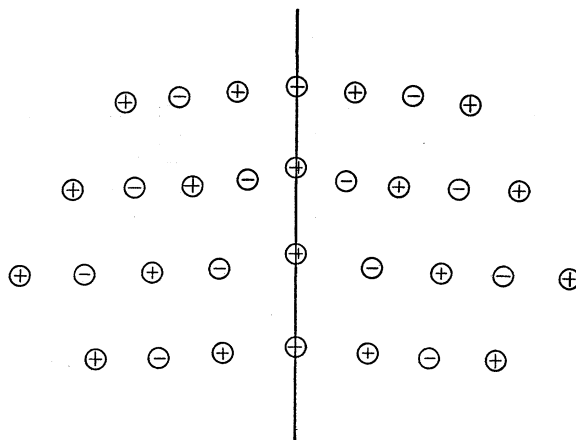


FIG. 13. Edge dislocation for slip in (100) plane. Positions are those given by the isotropic elastic theory.

preference for slip in the (110) planes exhibited by alkali-halide single crystals, since the elastic energy for an edge dislocation for slip in these planes is some 20% higher than for the edge dislocation for slip in the (100) planes. It is uncertain whether the active slip system is determined by the requirement of lowest barrier for dislocation motion or smallest energy per unit length for the appropriate edge dislocation. Believing that the second criterion might be important, we have attempted to estimate the core energy for the edge dislocation for (100) slip. This dislocation is shown in Fig. 13 with ion rows distributed according to the isotropic elastic solution, Eq. (8). One must be content with much more approximate methods here because of the disordered array of positive and negative rows. There is then no easy way to take into account exactly the effect of the long-range log terms. Instead, we have evaluated only a finite number of these, including arbitrarily only nine rows on each side of the slip plane. In estimating the energy of the dislocation four terms were taken into account (i) electrostatic interactions across the slip plane, (ii) ion-core interactions across the slip plane, (iii) short range interactions on the same side of slip plane, and (iv) logarithmic interactions on the same side of the slip plane.

(i) As a first step x -displacements only, corresponding to the elastic dislocation, Eq. (8) were considered. (Effect of y -displacements is small.) Because of complexities no attempt was made to apply variational refinements later. The electrostatic interactions across the slip plane were estimated by considering each atom in the plane directly above the slip to be in the field of a plane of alternating charges arranged in a square array at a distance a below. This potential is given by¹⁰

$$V(x,y,z) = (e/a) \exp(-\pi z/a) \times \cos(2\pi x/a) \cos(2\pi y/a), \quad (15)$$

where x and y are coordinates in the plane and z is perpendicular to the plane with the origin at the site

of a positive charge. On this basis, the electrostatic energy of the nine atoms just above the slip plane was found to be $0.24 e^2/a$, or 1.20 ev. For the nine atoms just below the slip plane the corresponding number was 0.88 ev. These two procedures for calculating the electrostatic energy of cross-plane interactions do not agree because Eq. (15) is only an approximation to the potential of the distorted planes. The arithmetic average, 1.04 ev was assumed.

(ii) In calculating the ion-core cross-plane interactions it was important for the first time to consider repulsions between ions of the same sign. Instead of using Eq. (10) we have reverted to the original Born-Mayer expression for the repulsive potential between ions 1 and 2,

$$W'(x) = 10^{-12} \text{ erg exp}[-(x-r_1-r_2)/\rho], \quad (16)$$

where the r_i are the radii of the ion cores. Huggins and Mayer's values¹⁴ were used; for sodium 0.875 Å and for chlorine 1.475 Å. The dislocation displacements increased the repulsions of the Cl-Cl bonds by 0.49 ev and lowered the repulsions of the Na-Cl bonds by 0.39 ev, giving a net increase of 0.10 ev for the cross-plane repulsions.

The Cl-Cl interaction depended slightly on configuration, i.e., on whether the dislocation center lay between two Cl ion rows or two Na ion rows. For the case of no relaxation allowed the difference was evaluated as 0.02 ev, i.e., the amount by which the chlorine-centered configuration lies above the sodium-centered configuration. It is rather unusual to be able to distinguish so clearly by numerical rather than analytic methods, the change in energy of a dislocation in moving half a lattice translation along the slip plane. The minimum resolved shear stress for a slowly moving dislocation to surmount such a sinusoidal barrier would be 2.2×10^9 dynes/cm², or over a thousand times the observed critical shear stress for annealed single crystals. While this value might be greatly reduced in the process of relaxation, it seems doubtful whether the edge dislocations in the (100) slip plane will be mobile for the range of critical shear stress that is experimentally observed.

(iii) The short-range interactions between adjacent rows on the same side of the slip plane is made up of the nonlog term in Eq. (13) and the ion-core repulsions [Eq. (16)], using $z=b/2$. Since the interactions were both repulsive, the energy in the upper half rose by 1.16 ev. Correspondingly, the energy of the ion rows below the slip plane fell by 0.64 ev, leaving a net 0.52 ev.

(iv) The logarithmic terms were calculated separately for both groups of ions. Labor was decreased and accuracy improved by taking analogous pairs above and below together and obtaining the logarithm of the ratio of the distances. The resultant of these terms is -0.31 ev.

Combining the results from all four parts, one obtains 1.73 ev/plane for this edge dislocation. This result may be in error by as much as 50 percent, not only because of the approximate methods used, but also because no variation of the position parameters has been employed to minimize the energy. Also, the selection of ion rows included has not been as systematic as before where the use of the concentric cylindrical surfaces made possible fitting to the elastic solutions at large R . If one takes 1.9 ev as the energy of 16 rows with $R=1.9a$, then the constant term for this dislocation (energy for $R=a$) is 1.5 ev, where the coefficient of $\ln(r_1/r_0)$ is taken to be 0.644 ev per plane (Tables II or VI).

It has been suggested¹⁵ that since the dislocations in NaCl have a Burgers vector which is slightly larger than the shortest distance between neighbors in the crystal, the cores of some types may be hollow.¹⁶ We may make an estimate of the size of the hollow by considering the crystal as a continuum, and assuming that the deleted material creates a surface tension. The radius of the hollow, if we use the elastic energies calculated earlier, turns out to lie between $\frac{1}{2}$ and 1 atomic distances for each of the three main types of dislocations possessing Burgers vector $[110]$. Hence the question essentially becomes one of determining the core configuration by means of r -wise relaxation. The work reported earlier shows that the "full" dislocation is at least a local minimum for displacements. However, calculations have not been done where a single line of atoms has been removed at the center of the core for comparison with the "full" core. One would expect on electrostatic grounds that hollows at the centers of dislocation lines with (110) slip planes will be easier to form than at the centers of the other two types. It is conceivable that removing the ion row directly above the center of the dislocation for Configuration I (Fig. 6) might lower the energy but it is difficult to see how this could be done for Configuration II (Fig. 7) without altering the symmetry. For this reason, it appears that such hollow dislocations, if they exist, would have low mobility.

IV. CONCLUSIONS

A summary of the results reported is given in Table VI.

Though the elastic calculations and those dealing with dislocation cores appear quite reliable and self-consistent within the framework of the mathematical model, the information they give does not afford a ready explanation of the physical facts of the plastic behavior of NaCl. A somewhat similar situation prevails here as for the f.c.c. metals, where the calculations of Foreman and Lomer¹⁷ have shown that the elastic energy per unit length of the edge dislocation in the observed slip planes (111) is higher than for those in the (110) planes. While in the case of the f.c.c. metals

¹⁵ J. S. Koehler (private communication).

¹⁶ F. C. Frank, *Acta Cryst.* 4, 497 (1951).

¹⁷ A. J. E. Foreman and W. M. Lomer, *Phil. Mag.* 46, 73 (1955).

¹⁴ M. L. Huggins and J. E. Mayer, *J. Chem. Phys.* 1, 643 (1933).

TABLE VI. Dislocation energies—values for A and B [see Eq. (12)].

	Slip plane	Burgers vector	A		B	
			ev/plane	10^7 ev/cm	ev/plane	10^7 ev/cm
80°K						
Edge	(110)	[110]	0.508	1.81	0.39	1.37
Edge	(100)	[110]	0.644	1.62	1.5	3.8
Screw		[110]	0.544	1.37	0.15	0.39
Edge	(010)	[002]	1.016	3.62		
Screw		[002]	0.586	2.09		
1000°K						
Edge	(110)	[110]	0.246	0.875		
Edge	(100)	[110]	0.377	0.950		
Screw		[110]	0.257	0.648		
Edge	(010)	[002]	0.492	1.75		
Screw		[002]	0.442	1.57		

the existence of extended dislocations in the (111) planes is the probable explanation of the preference for slip on these planes, there is little likelihood that extended dislocations are important for alkali halides.

Though a higher value for the dislocation core energy for the (100) slip plane seems clearly indicated from the preceding section, the difference might be considerably reduced by minimization. If one accepts the result calculated for the (100) cores at its face value and cuts off the logarithm term in the elastic energy at a value R corresponding to the distance between dislocations, then one finds that the difference in energy per unit length between the (100) and the (110) dislocations is

$$E_{100} - E_{110} = [2.4 + 0.19 \ln(\pi N)^{\frac{1}{2}}] \times 10^7 \text{ ev/cm}, \quad (17)$$

where N is the dislocation density. The energy difference goes to zero for N equal to $4 \times 10^8/\text{cm}^2$, a low value for dislocation density. For higher densities the energy difference would be positive but varies only slowly with N . In view of the uncertainty in the value for the core energy of the (100) dislocation, the small size of the energy difference found here is of doubtful significance in establishing any preference on the part of the edge dislocations for the (110) slip planes.

If dynamic considerations are dominant in determining the slip plane, one would naturally look to the form of the screw dislocation (Configuration III) for a hint as to the direction it will move most readily. Here the evidence from our model is disquieting since the distortion of the screw's shape from cylindrical symmetry is such as to favor motion in the close-packed plane. Moreover, the edge dislocation core investigated here appears quite concentrated. This tends to raise the barrier for dislocation motion and hence the critical shear stress higher than one would like.

On the other hand the calculations do indicate a high barrier for the motion of edge dislocations in the (100) slip plane, arising from the large repulsive interactions of the closed shells of the anions. In the limit in which one neglects the presence of the alkali atom altogether

the (100) plane ceases to be close-packed. This concept provides an intuitive basis for understanding why the anion repulsion prejudices so strongly the motion of edge dislocations in the (100) plane. Though the calculated value for barrier height reported here is not particularly reliable, the result appears to rule out the mobility of these dislocations at the lower applied stress levels. For materials with larger cations, such as the thallos salts, the situation might well become sufficiently changed to favor slip on other planes.

ACKNOWLEDGMENTS

It is a pleasure for the last-named author (R.T.) to acknowledge many stimulating discussions with Professor F. Seitz and Professor J. Koehler.

APPENDIX I. SUMMATION OF \ln POTENTIALS

We wish to develop an expression for the electrostatic potential of a rectangular array of parallel line charges, the lines being alternately positive and negative. The pattern of points formed in a plane perpendicular to the line charges will be an interlocking, face-centered lattice. In particular we are concerned with the curvature of the potential along the principal rectangular axes as experienced by one line charge moving in the field of all the others. Let the equilibrium position of this line be the origin, and, if the translation distances are $2f$ and $2g$, then the radial distance to any other particular line charge is given by

$$r = \{(ng)^2 + (mf)^2\}^{\frac{1}{2}}, \quad (\text{A-1})$$

when the integers n and m are the coordinates of the second line charge in the lattice. At a point ϵ from the origin along the f axis the potential is

$$V(\epsilon) = -2q \sum_{n=-\infty}^{\infty} \sum_{m=-\infty}^{\infty} (-1)^{n+m} \ln[(ng)^2 + (mf - \epsilon)^2]^{\frac{1}{2}}, \quad (\text{A-2})$$

where q is the charge per unit length, if $\epsilon \ll f$

$$\Delta V = V(\epsilon) - V(0)$$

$$\cong q \sum_{n=-\infty}^{\infty} \sum_{m=-\infty}^{\infty} (-1)^{n+m} \left[\frac{-2mf\epsilon + \epsilon}{r^2} - \frac{2m^2f^2\epsilon^2}{r^4} \right]. \quad (\text{A-3})$$

The linear term in ϵ will drop out because its coefficient is odd in m . It can be shown¹⁸ that

$$\sum_{n=1}^{\infty} \frac{(-1)^n}{n^2 + k^2} = \frac{\pi}{2k} \operatorname{csch}(k\pi) - \frac{1}{2k^2}$$

and

$$\sum_{m=1}^{\infty} \frac{m^2(-1)^m}{(m^2 + d^2)^2} = \frac{\pi}{4d} \left[\frac{\sinh(d\pi) - (d\pi) \cosh(d\pi)}{\sinh^2(d\pi)} \right]; \quad (\text{A-4})$$

¹⁸ For an ingenious method of handling such summations see M. R. Spiegel, *J. Appl. Phys.* **23**, 906 (1952).

consequently

$$\Delta V \cong -q\epsilon^2 \left\{ \left[\frac{2\pi}{fg} \sum_{m=1}^{\infty} (-1)^m \frac{\operatorname{csch}(mf\pi/g)}{m} - \frac{2\pi^2}{12g^2} \right] + \left[\frac{4\pi^2}{12f^2} - \frac{2\pi}{fg} \sum_{n=1}^{\infty} \frac{(-1)^n}{n} \right] \times \left(\frac{\sinh(ng\pi/f) - (ng\pi/f) \cosh(ng\pi/f)}{\sinh^2(ng\pi/f)} \right) \right\}. \quad (\text{A-5})$$

For present application, $q = e/b$, $f = b/2$ and $g = b/\sqrt{2}$ so

that

$$\Delta V = -\frac{2e}{b} \left(\frac{\epsilon}{b} \right)^2 \left\{ \frac{\pi^2}{2} + 2\pi\sqrt{2} \left[\sum_{n=1}^{\infty} \frac{(-1)^n}{n} \left(\operatorname{csch} \frac{\sqrt{2}\pi n}{2} + \frac{(\sqrt{2}\pi n) \cosh(\sqrt{2}\pi n) - \sinh(\sqrt{2}\pi n)}{\sinh^2(\sqrt{2}\pi n)} \right) \right] \right\}.$$

The series in the square bracket converges very rapidly so that the third term is 0.3% of the first. The final result is

$$\Delta V(\epsilon) \cong -4.76 \frac{e}{b} \left(\frac{\epsilon}{b} \right)^2. \quad (\text{A-6})$$

Longitudinal Photomagnetolectric Effect in Germanium

JACK ARON AND GERHART GROETZINGER

Lewis Flight Propulsion Laboratory, National Advisory Committee for Aeronautics, Cleveland, Ohio

(Received June 27, 1955)

The emf developed parallel to the gradient of light absorption (Dember emf) in a germanium crystal is reduced by the application of a transverse magnetic field, the diminution being about 10% for a field of 5000 gauss. The size of the effect is approximately quadratic in the field up to about 2000 gauss, is then linear to 4000 gauss, and subsequently saturates.

IT was found earlier by one of us¹ that the photo-emf developed along the direction parallel to the gradient of light absorption in an illuminated cuprous oxide crystal² is reduced by the application of a (transverse) magnetic field. In view of the fact that germanium is one of the few elements which are intrinsic semiconductors it seemed of interest to determine whether such an effect exists in this material.

A piece of high-purity polycrystalline *n*-type germanium (resistivity: 50 ohm cm at room temperature)³ of dimensions 8×8×5 mm was etched in a CP4 solution.⁴ It was then placed between the poles of an electromagnet in such a way that the field was parallel to an 8-mm edge and that one of the 8×8 mm faces could be illuminated by a Bausch and Lomb Microscope Illuminator equipped with a 6-v, 18-amp bulb. A point contact of Inconel was held against each 8×8 mm face by spring pressure, the arrangement being such that the position of the point of each contact on the face could be altered. The emf between the two contacts was measured with a potentiometer. A difficulty in looking for the effect described above arises because application of a magnetic field transverse to the light

gradient in germanium^{5,6} produces an emf along a direction normal to both the field and the gradient. To reduce the contribution of this origin to the emf measured here with the field applied, the crystal was illuminated and the position of the contacts adjusted in such a fashion that the application of a low (250-gauss) magnetic field⁷ in either direction produced essentially no change in the emf between them.

With the contacts thus aligned, it was found that the application of a sufficiently high magnetic field in either direction caused a decrease in the emf, e , between the

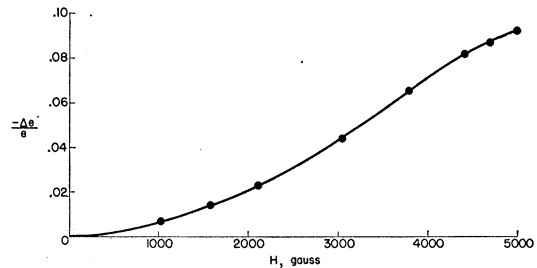


FIG. 1. Longitudinal photomagnetolectric effect in germanium as a function of the magnetic field strength.

¹ G. Groetzinger, *Physik. Z.* **36**, 169 (1935); **36**, 216 (1935).

² H. Dember, *Physik. Z.* **33**, 207 (1932).

³ We are indebted to Dr. M. Selker of the Clevite-Brush Development Company who kindly provided us with the germanium.

R. D. Heidenreich, U. S. patent No. 2619414 (1952).

⁵ P. Aigrain and H. Bulliard, *Compt. rend.* **236**, 595 and 672 (1953).

⁶ H. Bulliard, *Phys. Rev.* **94**, 1564 (1954).

⁷ Since the effect sought can be expected to produce a change in the emf proportional to H^2 for small values of H while the interfering emf goes linearly with H , it follows that at sufficiently low values of H only the latter effect will be appreciable.